NANO EXPRESS

Facile Phosphine-Free Synthesis of CdSe/ZnS Core/Shell Nanocrystals Without Precursor Injection

Chang-Qing Zhu · Peng Wang · Xin Wang · Yan Li

Abstract A new simple method for synthesis of core/shell CdSe/ZnS nanocrystals (NCs) is present. By adapting the use of cadmium stearate, oleylamine, and paraffin liquid to a non-injection synthesis and by applying a subsequent ZnS shelling procedure to CdSe NCs cores using Zinc acetate dihydrate and sulfur powder, luminescent CdSe/ZnS NCs with quantum yields of up to 36% (FWHM 42–43 nm) were obtained. A seeding-growth technique was first applied to the controlled synthesis of ZnS shell. This method has several attractive features, such as the usage of low-cost, green, and environmentally friendlier reagents and elimination of the need for air-sensitive, toxic, and expensive phosphines solvent. Furthermore, due to one-pot synthetic route for CdSe/ZnS NCs, the approach presented herein is accessible to a mass production of these NCs.

Introduction

Colloidal semiconductor nanocrystals (NCs) are of great interest for both fundamental studies [1, 2] and technical applications such as light-emitting devices [3, 4], lasers [5, 6], and fluorescent labels [7–9]. CdSe nanocrystals have become the most extensively investigated NCs due to their size-dependent photoluminescence tunable across the visible spectrum [10]. Recently, much experimental work has been devoted to molecular surface modification to improve the luminescence efficiency [11, 12] and photostability of the NCs or to develop a reliable processing chemistry [13, 14]. To attain the ends, overcoating NCs with another wide band gap semiconductor is a well-established method [11, 15–17]. In particular, for CdSe NCs the particles were covered with ZnS [15, 17] to establish a core/shell system, where the band gap of the core lies energetically within the band gap of the shell material and the photogenerated electrons and holes are mainly confined inside the CdSe. Such core/shell NCs have widespread applications in biological and biomedical research [7–9, 18] due to their better stability and processibility. In addition, with the growing interest in applications based on these nanoscale materials comes a need for their large-scale synthesis.

So far, the methods for synthesis of NCs, described in the literature, are too many and variable. The most successful and widely used nanocrystal synthesis relies on rapid precursor injection [19–21]. Meanwhile, non-injection-based synthesis method has also been employed for mass production of NCs in recent years. One noteworthy study was the one-pot synthesis of CdS NCs reported by Cao et al. [22]. Also, continued research on synthesis of NCs without precursor injection has successfully achieved making CdSe and CdTe NCs [23]. This strategy mainly focused on synthesis of core NCs. In fact, in the case of core/shell NCs, one-pot synthetic approach proposed by Weller et al., where both core and shell can grow controllably in the same reaction mixture, has been applied to fabricate CdSe/CdS NCs [24]. For the synthesis of CdSe/ZnS NCs, numerous approaches based on one-pot synthetic method have been exploited, such as ultrasonic baths [25], the use of single molecular precursors [26], and microwave-supported synthesis [27]. However, until recently it was not possible to eliminate phosphines as coordinating solvents from the synthesis

C.-Q. Zhu (✉) · P. Wang · X. Wang · Y. Li
College of Chemistry and Materials Science, Anhui Key Laboratory of Functional Molecular Solid, Anhui Normal University, Wuhu 241000, Peoples Republic of China
e-mail: zhucq@mail.ahnu.edu.cn

procedure. For example, trioctylphosphine (TOP) or tribu-tylphine (TBP) was ubiquitously used to dissolve Se precursor or shell precursors in the process of synthesis of NCs. In fact, the costs of large-scale synthesis of NCs are still very high because of using expensive solvents such as TOP (or TBP). Additionally, TOP (TBP) is hazardous, unstable, and not an environmentally friendly solvent [28]. In this article, we are interested in the preparation of this core/shell NCs from inexpensive, stable starting materials of low tox-icity via a greener chemistry route. Here a one-pot synthesis of CdSe/ZnS NCs without phosphines is reported, using zinc acetate dihydrate and sulfur powder as shell precursor and paraffin liquid as solvent, based on a modified non-injection method for the synthesis of CdSe core NCs. Compared with the former methods [24–26], the precursors we used are low-cost, clean, and air/water-stable. Moreover, we adopt a seeding-growth technique to mediate the growth of ZnS shell. So, controllable shell growth can be favorably achieved without coordinating solvents such as TOP. The seeding-growth technique has been applied to synthesize CdS NCs by Ji and An et al. [29]. In this article, it is first used for synthesis of core/shell NCs. The CdSe/ZnS NCs reported here exhibit considerable improvement of PL and relative monodispersity. Furthermore, the CdSe/ZnS NCs synthe-sized by the new route have a different crystal structure from those made by precursor injection methods [19–21] (zinc blande vs wurtzite, respectively), which would make these NCs possess some special properties.

Experimental Section

Materials

All chemicals were used as received without further puri-fication. Cadmium oxide (CdO, Aldrich, 99.5%), selenium powder (Se, Aldrich, 95%), oleylamine (OA, Aldrich, 70%) were used in the preparations described here. Paraffin liquid (chemical grade), stearic acid (analytical grade), Zinc acetate dihydrate ($Zn(OAc)_2 \cdot 2H_2O$, analytical grade), sulfur powder (S, analytical grade), n-hexane (analytical grade), methanol (analytical grade), and acetone (analytical grade) were obtained from Sinopharm chemical Reagent Co., Ltd, China. Rhodamine B was purchased from Alfa Aesar.

Synthesis of CdSe Core QDs

Cadmium stearate was prepared by heating the mixture of CdO and Stearic acid at 220 °C for 12 min. The crude product was recrystallized twice from toluene and then used for further reaction. A typical synthesis procedure of CdSe NCs is given briefly below. Se powder (0.0039 g,

0.05 mmol) and cadmium stearate (0.0679 g, 0.1 mmol) were added into a three-neck flask with 8 mL paraffin liquid. The mixture was degassed in vacuum for 15 min at room temperature and then heated under N_2 to 225 °C with oil-bath heating for reaction. Aliquots were taken from the reaction mixture to monitor the growth of core NCs. After 2.5 min, 1.5 mL OA was added dropwise into the mixture to stabilize the growth of the NCs. The mixture was cooled naturally to ambient temperature when NCs with desirable size were obtained. Because Cadmium stearate was solid-ified from paraffin liquid at room temperature, the crude core solution was only simply purified by direct centrifu-gation at a low speed. Cadmium stearate separated from the solution can be used for synthesis of CdSe NCs.

Synthesis of CdSe/ZnS NCs

Typically, the resulting core solution (reaction for 3 min), $Zn(OAc)_2 \cdot 2H_2O$ (0.085 mmol) and S powder (0.085 mmol) were mixed together in the reaction vessel. The reaction volume was adjusted to 15 mL by adding paraffin liquid. Next, with stirring, the mixture was degassed at 80 °C for 20 min. Afterward, temperature was set to 145 °C for the shell growth under N_2 atmosphere. To monitor the reaction, aliquots were taken at different times. The reaction mixture was cooled to room temperature after 50 min. To grow shell ZnS with different thicknesses around a CdSe core, a seeding-growth technique [29] was applied. The same amount of Zn and S precursors as the first shell precursors as added to the reaction mixture and further shelling was done. This shell growth cycle was repeated until desired core–shell NCs were obtained. Finally, the CdSe/ZnS NCs were precipitated by the addition of acetone, then separated, and finally redispersed for further processing.

Characterization

The nanocrystal solutions were dropped onto copper grids with carbon support by slowly evaporating the solvent in air at room temperature. The ultra structure of the nano-crystals was examined using a JEOL 2010 transmission electron microscope operating at 200 kV. X-ray diffraction patterns were recorded using powder X-ray diffraction measurements (XRD, Rigaku D/max-b) using Cu Kα radiation (λ = 1.5406 Å). The X-ray photoelectron spectra (XPS) were taken on a VG ESCALAB MK Π electron energy spectrometer using Mg Kα (1253.6 eV) as the X-ray excitation source. Ultraviolet and visible absorption (UV–vis) spectrum was recorded with a Hitachi U-3010 spec-trophotometer (Tokyo, Japan) at room temperature. PL spectroscopy investigations were carried out on a fluores-cence spectrophotometer FL 4500 (Tokyo, Japan) using a

150 W xenon lamp as the excitation source. The aliquots were diluted with *n*-hexane directly for characterization without any size sorting. The PL QYs of NCs were estimated following the procedure used previously [26, 28] by comparison with Rhodamine 6G in methanol, assuming its PL QYs as 95%, and using data derived from the luminescence and the absorption spectra as the following:

$$\Phi = \Phi_s \left(\frac{I}{I_s}\right)\left(\frac{A_s}{A}\right)\left(\frac{n^2}{n_s^2}\right)$$

In this equation, I (sample) and I_s (standard) are the integrated emission peak areas, upon 480 nm excitation; A (sample) and A_s (standard) are the absorption at 480 nm; n (sample) and n_s (standard) are the refractive indices of the solvents; and Φ and Φ_s are the PL QYs for the sample and the standard, respectively.

Results and Discussion

Low-cost and green reagents were used for the synthesis of CdSe/ZnS NCs. Herein, paraffin liquid was selected as the solvent. It is a colorless liquid at room temperature, boiled at above 300 °C, and environmentally friendly. Also, that it is cheaper than octadecene. The CdSe NCs were synthesized by using modifications of previously reported method [23]. In our experiments, we set the temperature of reaction at 225 °C, because at this temperature the activity of fatty acid cadmium salts was high enough and Se powder was completely dissolved [23]. To avoid aggregation of CdSe NCs, OA was added to the growth solution after heating for 2.5 min. It must be pointed out that OA should be added to the reaction mixture after CdSe NCs have formed, in case the toxic H_2Se is released resulting from the reaction of OA and Se powder at this high temperature. Figure 1 shows the emission spectra (normalized to the first emission maximum) of CdSe NCs taken at different time intervals. At the time indicated, a sample was taken from the hot reaction mixture and diluted into 2 mL of *n*-hexane. The emission peaks of CdSe NCs range from 513 to 594 nm, and the corresponding full width at half-maximum (FWHM) of the band-edge luminescence was maintained between 37 and 55 nm. The PL peak shifts to longer wavelength with increasing CdSe sizes as a consequence of quantum confinement. The Fig. 2a shows the emission and absorption spectra of the OA-capping CdSe NCs taken from reaction mixture after 3 min. The absorption spectrum shows the sharp first excitonic peak (at 534 nm), indicating a relative narrow size distribution of the resulting NCs. The band-edge emission of CdSe NCs is 551 nm, and the corresponding full width at half-maximum (FWHM) of the band-edge luminescence is around 46 nm. The room temperature PL QY of core NCs is 1.2%. The size of CdSe
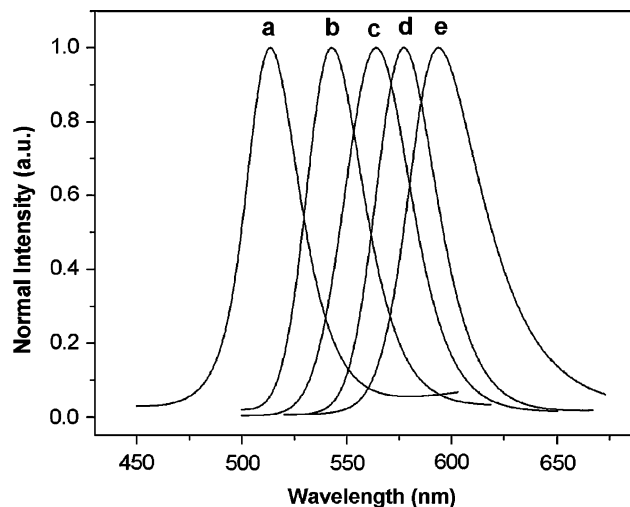

Fig. 1 Normalized PL spectra of CdSe NCs from the same solution, as function of time: (**a**) 0.5 min, λ_{max}: 513 nm; (**b**) 2.5 min, λ_{max}: 543 nm; (**c**) 3.5 min, λ_{max}: 564 nm; (**d**) 4 min, λ_{max}: 577 nm; (**e**) 5 min, λ_{max}: 594 nm

NCs was approximately 2.8 nm, calculated from the first excitonic peak position according to the literature [30]. Furthermore, the TEM image shown is Fig. 2b indicates monodispersed core NCs. The size of as-prepared NCs determined from TEM image is 2.8 nm, which is consistent with the former calculation.

As mentioned earlier, the formation of a semiconductive shell over a NCs core structure greatly enhances the photophysical properties of the NCs. ZnS has a wide band gap (3.68 eV) as compared to the CdSe (band gap of 1.7 eV) at 300 K [31]. So ZnS is the commonly used capping agent for CdSe NCs.

It is important to search for a matching shell precursor for shelling of core NCs. In principle, the reactivity of the precursors should be weak enough to prevent independent nucleation, but sufficiently strong to promote the epitaxial growth around the existing core NCs [16]. Therefore, it is essential that the shell grew epitaxially below the temperature of core growth. To grow a shell ZnS around a CdSe core, highly toxic Zn and S precursors such as diethylzinc and hexamethyldisilathiane are commonly added to the washed CdSe NCs [17]. Here, we have found that heating $Zn(OAc)_2 \cdot 2H_2O$ and S powder at 145 °C can accomplish the efficient ZnS shelling of CdSe NCs; meanwhile the growth of core NCs hardly occurred. In our synthesis, no attempts were made to remove the remaining precursors of CdSe NCs synthesis or excess ligands by prior washing steps. Instead, we just simply purified the core nanocrystals through centrifugation to remove the Cd-stearate solidified from core solution, for the sake of the optical characterization of core and core/shell nanocrystals. In fact, growth of a CdS shell would not occur even if a slightly excess or

Fig. 2 Normalized PL and absorbance spectra (**a**), and TEM overview image with size distribution histograms pattern (**b**) of 2.8 nm CdSe core NCs
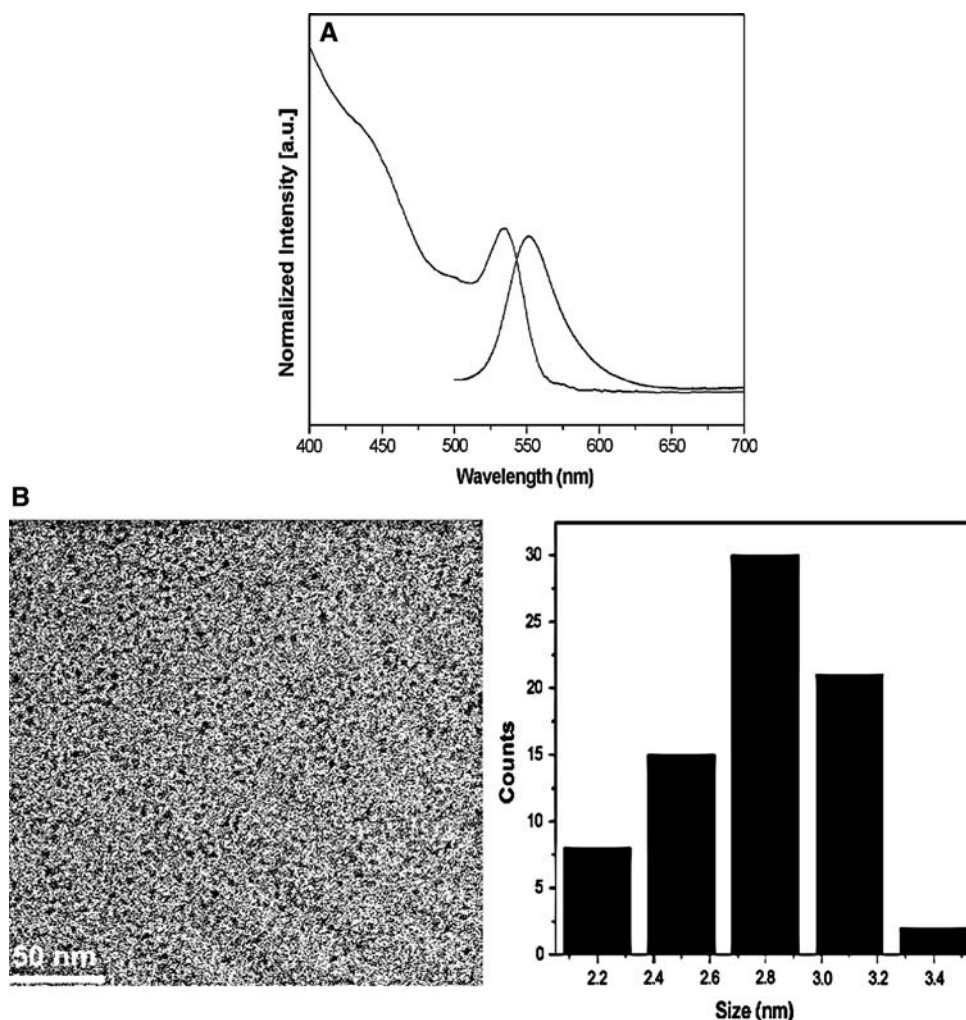
non-reacted Cd-stearate exists in the core solution, due to the low activity of Cd-stereate at the temperature of shell growth, which can be confirmed by the XPS data. This one-pot approach is not only less laborious but also ensures the same undisturbed ligand coverage and homogeneous distribution of NCs in the matrix for each synthesis [27]. Surprisingly, a little water existing in Zn precursor plays an important role in the shelling reaction. It should be noted that the reaction did not carry out well when $Zn(OAc)_2 \cdot 2H_2O$ was replaced by $Zn(OAc)_2$ dehydrate. Experimental result indicated that the solubility of $Zn(OAc)_2$ dehydrate was lower than $Zn(OAc)_2 \cdot 2H_2O$ in paraffin liquid at this temperature. This result may be ascribe to a little of acidic or basic compound in the paraffin liquid, which enhances the solubility of $Zn(OAc)_2 \cdot 2H_2O$. Therefore, $Zn(OAc)_2 \cdot 2H_2O$ was used as Zn precursor. Furthermore, the usage of such cheap, stable, and available materials and one-pot synthetic method embodies the concept of a facile and green synthesis. To avoid the homogeneous nucleation of the shell materials, a seeding-growth technique [29] was applied, in which a certain

amount of Zn and S precursors were added each time (see experimental section for details). During the shelling process, a fresh mixture of the shell precursors was mixed with the original reaction medium containing the core NCs for the completion of the first shell growth reaction, and the resulting NCs were denoted as "a" and used as "core" NCs for the next growth reaction. The reaction time used here for shell growth reactions is 50 min. This shell growth cycle was repeated by using NCs from the previous cycle as "core" NCs, and the resulting NCs were denoted, respectively, as "b, c, e" in sequence (sample d was recorded in the fourth shell growth reaction shown in Fig. 3 and Table 1). Note that this shelling procedure eliminates alternate injection of shell precursors and adopts one-pot synthetic route, which is different from the SILAR technique developed by Peng et al. [16]. The growth dynamics of CdSe/ZnS NCs was monitored by the UV–Vis absorption spectra shown in Fig. 3a. As the thickness of the ZnS shell increases, the absorption peaks are slightly red-shifted and the broadening of the absorption peak increases, resulting from an increased leakage of the exciton into the shell [17].

Fig. 3 Evolution of (**a**) absorption and (**b**) PL spectra of as-prepared CdSe/ZnS NCs with increasing shell growth cycle
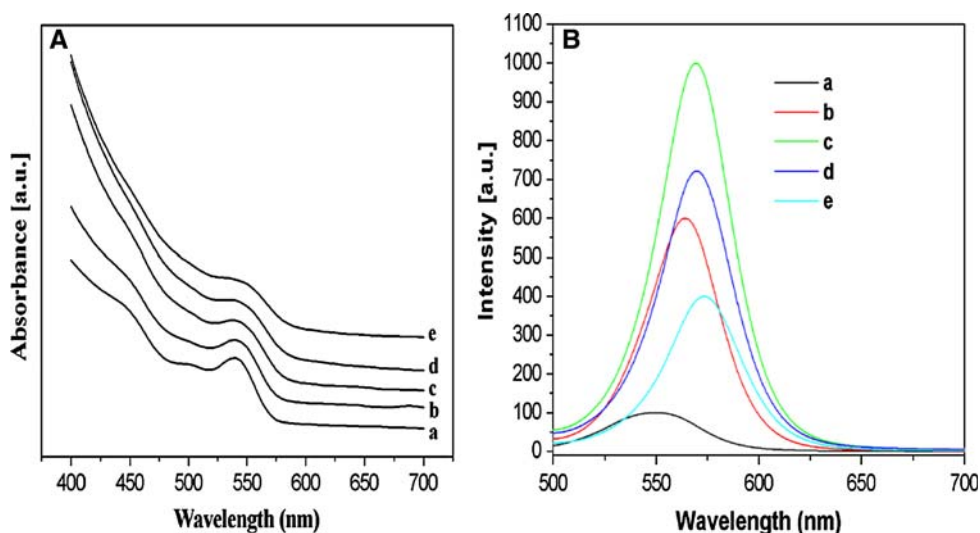

Table 1 PL FWHM, peak site, and QYs of CdSe/ZnS NCs for varying shell growth cycles

|	Cycles of reaction (times)	Sample	Reactions[a] time (min)	FWHM (nm)	Peak site (nm)	QYs (%)
CdSe/ZnS	1	a	50	53.4	551.9	4
	2	b	50	42	563.8	25
	3	c	50	42.4	569.4	36
	4	d	20	42.6	570.4	29
		e	50	43.2	573.4	22

[a] Aliquots were taken at different times for monitoring the reaction of shelling every cycle. As the number of samples is high, here we have selected the representative ones

The evolution of the PL for the CdSe/ZnS NCs is displayed in Fig. 3b. It is obviously observed that the peak shape of PL (sample b) becomes more symmetrical than that of sample a. Further detailed data collected for PL of as-obtained core/shell NCs are shown in Table 1. As the cycles of shell growth increase, the red-shift of PL peak of as-prepared samples accompanied by a broadening of PL FWHM (except sample a) is observed. For the sample a, the PL FWHM is broadened when compared to that of CdSe core NCs (46 nm) and sample b (42 nm), respectively, suggesting a broadening of the size distribution during the first growth cycle. This phenomenon can illuminate the fact that the ZnS shell has grown epitaxially on the surface of the core NCs. However, with the continued shell growth, it is found that all the PL peaks have narrow FWHM (42–43 nm), which appeared to be comparable with that of CdTe/CdS NCs synthesized in water phase via a microwave-assisted route [32]. The narrow FWHM indicates the core/shell NCs have relative monodispersity as shown in the TEM spectrum (Fig. 4a). Moreover, as it shown, the PL QYs reach a maximum value (36%) upon the third shell growth cycle, after which a decrease in emission efficiency

is observed. The maximum emission efficiency has been attributed to a core/shell system, which has a completed ZnS shelling [33]. The slight decrease in QYs occur after reaction for additional shell growth cycle is because further increase in thickness of an already complete NCs shell reduces QYs [17, 33].

Figure 4 displays TEM and HRTEM images of the CdSe/ZnS core/shell NCs. It can be observed that the NCs have a narrow size distribution. Furthermore, the ZnS shell thickness can be estimated by the subtraction of the core size (observed in Fig. 2b) from that of the present prepared core/shell particles. The average diameters of CdSe/ZnS core/shell NCs, as measured by HRTEM, are 4.5 nm. Therefore, the average shell thickness is about 1.7 nm, which corresponds to 2.7 monolayer shells estimated using the distance (0.31 nm) between the adjacent lattice fringes along the ZnS (111) plane. The clear lattice plane observations on the HRTEM are indicative of the good crystallinity. Although the mismatch of the lattice constants between core (CdSe) and shell (ZnS) is 12%, it is impossible to allow the resolution of the core and shell individually via the difference in the lattice orientations

Fig. 4 TEM (**a**) and HRTEM (**b**) micrographs of CdSe/ZnS NCs (sample e in the Table 1) with 2.8 nm CdSe core NCs
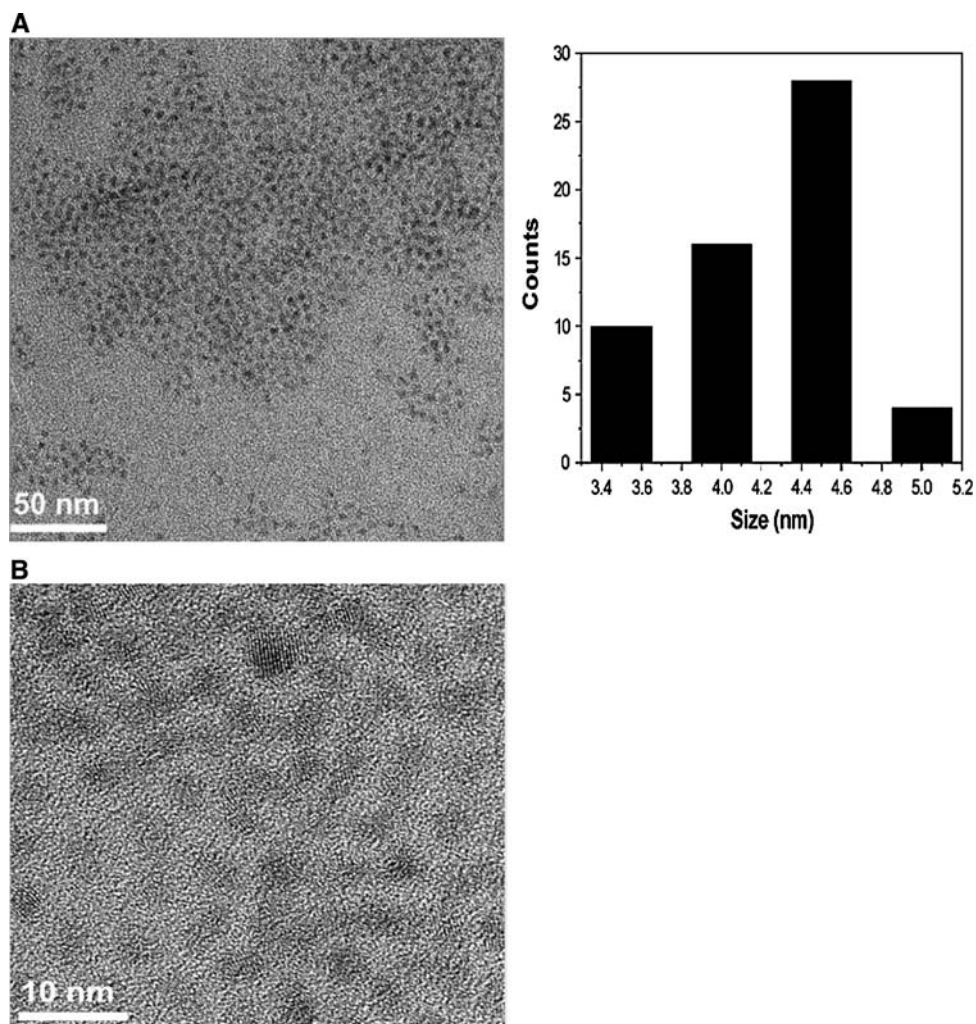
using TEM. This phenomenon has also been reported in many other types of core/shell NCs [15, 17, 24].

XRD patterns for 2.8 nm CdSe core NCs and the corresponding CdSe/ZnS core/shell NCs with 2.7 monolayer shells are shown in Fig. 5. After passivating ZnS shell, the diffraction pattern of CdSe moved slightly toward higher angles, which supports the formation of ZnS shell on CdSe. Figure 5 compares the diffraction patterns of CdSe cores with CdSe/ZnS core/shell. Two diffraction peaks corresponding to the (111), (200), and (311) lattice planes of the CdSe cores match those of the bulk CdSe cubic (zinc blende) peaks. The peaks are broadened because of the finite size of the nanocrystals. Upon the growth of the ZnS shell, peak positions shift to higher scattering angle, toward the positions of the bulk ZnS zinc blende peaks. The CdSe/ZnS NCs prepared by most injection-based approaches are usually hexagonal in structure, while those prepared by our route are cubic in structure. The mean crystalline sizes are 2.75 (for core NCs) and 2.78 nm (for core/shell NCs), respectively, calculated from (111) reflection by the

Scherrer formula. From the above data, it can be seen that the discrepancy of crystalline size between core and core/shell NCs is tiny, much lower than that observed from the TEM data, since the shell layer does not affect the XRD peak width from core [11, 34].

To further characterize the core/shell nanostructures, we carried out XPS to investigate the surface compositions and chemical state of CdSe and CdSe/ZnS core/shell NCs, and the results are shown in Fig. 6a and b, respectively. In our system, the CdSe and CdSe/ZnS core/shell NCs are capped with oleylamine, and therefore, the XPS lines of C 1s and O 1s are present in Fig. 6a and b. Similar phenomenon has been observed in ZnS NCs capped with oleylamine [35]. The two strong peaks located at 405.2 and 412 eV in Fig. 6a correspond to the Cd 3d binding energy of CdSe, while the peak at 54.3 eV corresponds to the Se 3d binding energy of CdSe. These results are close to that of bulk CdSe. The XPS spectrum of CdSe/ZnS core/shell NCs shows typical peaks for ZnS, with Zn 2p3/2 and S 2p3/2 located at 1022 and 161.5 eV, respectively. Furthermore,
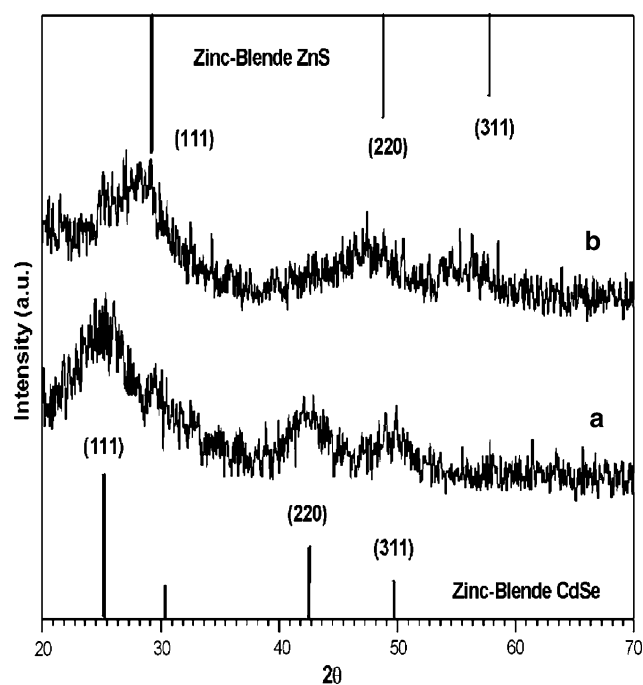
Fig. 5 The XRD patterns of the as-prepared (**a**) 2.8 nm CdSe core and (**b**) CdSe/ZnS NCs (sample e in the Table 1). The vertical bars correspond to (up) JCPDS file No. 77-2100 and (down) JCPDS file No. 19-0191, respectively

accurate quantitative compositions of Cd/Se and Zn/S in XPS were obtained by integrating the peak area and dividing by the atomic sensitivity factors [36]. The Cd/Se and Zn/S ratios from Fig. 6a and b are 1.2:1 and 1.3:1, respectively. Based on the XPS data, the growth of ZnS on CdSe NCs is confirmed.

Conclusions

In summary, we have developed a low-cost and non-phosphine-based approach for growing CdSe/ZnS core/shell NCs with zinc blende crystalline structure. We have found that a little water contained in Zn precursors play an important role in the preparation of the resulting NCs. By using a seeding-growth technique, the relative monodispersed CdSe/ZnS NCs were prepared. Compared with the traditional route, this method can be performed at relatively low temperature without the need for precursor injection. In addition, this approach may be applied to the synthesis of other core/shell NCs. The structure of CdSe/ZnS core/shell NCs is confirmed by TEM, XRD, and XPS. The as-prepared core/shell with enough high QYs is used potentially for bio-applications. Moreover, further work for digging out the properties and applications of such NCs is under way.
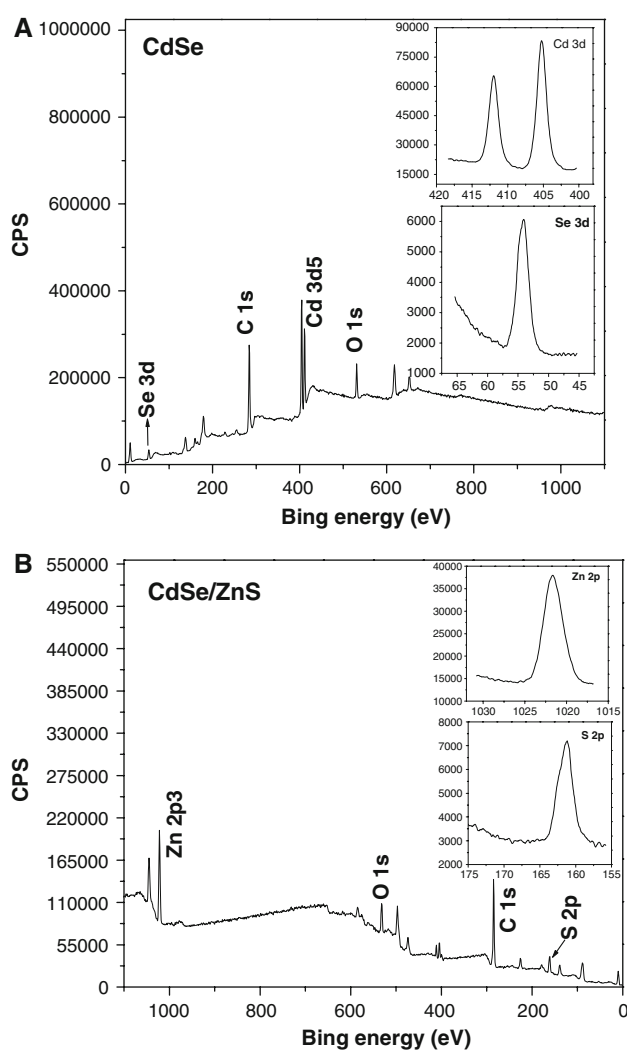

Fig. 6 XPS survey scans spectra of (**a**) 2.8 nm CdSe core NCs and (**b**) corresponding CdSe/ZnS core/shell NCs with 2.7 ZnS monolayers

References

1. N.C. Greenham, X. Peng, A.P. Alivisatos, Phys. Rev. B **54**, 17628 (1996)
2. S. Empedocles, M.G. Bwendi, Acc. Chem. Res. **32**, 389 (1999)
3. S. Coe, W.K. Woo, M. Bawendi, V. Bulovic, Nature **420**, 800 (2002)
4. R.A.M. Hikmet, D.V. Talapin, H. Weller, J. Appl. Phys. **93**, 3509 (2003)
5. C.E. Finlayson, D.M. Russell, C.M. Ramsdale, D.S. Ginger, C. Silva, N.C. Greenham, Adv. Funct. Mater. **12**, 537 (2002)
6. M. Kazes, D.Y. Lewis, Y. Ebenstein, T. Mokari, U. Banin, Adv. Mater. **14**, 317 (2002)
7. M. Bruchez, M. Moronne, P. Gin, S. Weiss, A.P. Alivisatos, Science **281**, 2013 (1998)

8. W.C.W. Chan, S.M. Nie, Science **281**, 2016 (1998)

9. A.R. Clapp, I.L. Medintz, J.M. Mauro, B.R. Fisher, M.G. Bawendi, H. Mattoussi, J. Am. Chem. Soc. **126**, 301 (2004)

10. R.G. Xie, U. Kolb, J.X. Li, T. Bashine, A. Mews, J. Am. Chem. Soc. **127**, 7480 (2005)

11. X.G. Peng, M.C. Schlamp, A.V. Kadavanich, A.P. Aivisatos, J. Am. Chem. Soc. **119**, 7019 (1997)

12. O.I. Micic, B.B. Smith, A.J. Nozik, J. Phys. Chem. B. **104**, 12149 (2000)

13. Y.A. Wang, J.J. Li, H.Y. Chen, X.G. Peng, J. Am. Chem. Soc. **124**, 2293 (2002)

14. J. Aldana, Y.A. Wang, X.G. Peng, J. Am. Chem. Soc. **123**, 8844 (2001)

15. M.A. Hines, P. Guyot-Sionnest, J. Phys. Chem. B **100**, 468 (1996)

16. J.J. Li, Y.A. Wang, W.Z. Guo, J.C. Keay, T.D. Mishima, M.B. Johnson, X.G. Peng, J. Am. Chem. Soc. **125**, 12567 (2003)

17. B.O. Dabbousi, J. Rodriguez-Viejo, F.V. Mikulec, J.R. Heine, H. Mattoussi, R. Ober, K.F. Jensen, M.G. Bawendi, J. Phys. Chem. B **101**, 9463 (1997)

18. I.L. Medintz, A.R. Clapp, H. Mattoussi, E.R. Goldeman, B. Fisher, J.M. Mauro, Nat. Mater. **2**, 630 (2003)

19. C.B. Murray, D.J. Norris, M.G. Bawendi, J. Am. Chem. Soc. **115**, 8706 (1993)

20. X.G. Peng, J. Wickham, A.P. Alivisatos, J. Am. Chem. Soc. **120**, 5343 (1998)

21. Y. Cao, U. Brain, J. Am. Chem. Soc. **122**, 9692 (2000)

22. Y.C. Cao, J.H. Wang, J. Am. Chem. Soc. **126**, 14337 (2004)

23. Y.A. Yang, H.M. Wu, K.R. Williamas, Y.C. Cao, Angew. Chem. Int. Ed. **44**, 6712 (2005)

24. I. Mekis, D.V. Talaphin, A. Kornowski, M. Haase, H. Weler, J. Phys. Chem. B **107**, 7454 (2003)

25. M.J. Murcia, D.L. Shaw, H. Woodruff, C.A. Naumann, B. Young, E.C. Long, Chem. Mater. **18**, 2219 (2006)

26. S.L. Cumberhand, K.M. Hanif, A. Javier, G.A. Khitrov, G.F. Strouse, S.M. Woessner, C.S. Yun, Chem. Mater. **14**, 1576 (2002)

27. J. Ziegler, A. Merkulov, M. Grabolle, U. Resh-Genger, T. Nann, Langmuir **23**, 7751 (2007)

28. Z.T. Deng, L. Cao, F.Q. Tang, B.S. Zou, J. Phys. Chem. B **109**, 16671 (2005)

29. Q. Wang, D.C. Pan, S.C. Jiang, X.L. Ji, L.J. An, B.Z. Jiang, Chem. Eur. J. **11**, 3843 (2005)

30. W.W. Yu, L.H. Qu, W.Z. Guo, X.G. Peng, Chem. Mater. **15**, 2854 (2003)

31. A. Kortan, R. Hull, R. Oplila, M.G. Banwendi, M. Streigerwald, P. Carroll, L. Brus, J. Am. Chem. Soc. **112**, 1327 (1990)

32. Y. He, H.T. Lu, L.M. Sai, W.R. Lai, Q.L. Fang, L.H. Wang, W. Huang, J. Phys. Chem. B **110**, 13370 (2006)

33. A. Baranov, Y. Rakovich, J. Donegan, T. Perova, R. Moore, D. Talapin, A. Rogach, Y. Masumoto, I. Nabiev, Phys. Rev. B Condens. Matter Mater. Phys. **68**, 165306 (2003)

34. L. Manna, E.C. Scher, L. Li, A.P. Alivisotos, J. Am. Chem. Soc. **124**, 7136 (2002)

35. Z.W. Quan, Z.L. Wang, P.P. Yang, J. Lin, J.Y. Fang, Inorg. Chem. **46**, 1354 (2007)

36. H. Yang, P.H. Holloway, Adv. Funct. Mater. **14**, 152 (2004)